Bull. Chem. Soc. Jpn., 73, 1919—1923 (2000) 1919

High Magnetic Field Effects on Interdigitated Microarray Electrodes

Satoko Nishiyama and Ryoichi Aogaki*,†

National Research Laboratory for Magnetic Science, Japan Science and Technology Corporation,
1-1-56 Shibashimo, Kawaguchi, Saitama 333-0848

†Department of Product Design, Polytechnic University, 4-1-1, Hashimoto-dai, Sagamihara, Kanagawa 229-1132

(Received March 2, 2000)

High magnetic field effects were determined for a typical electrochemical reaction, the oxidation of hexacyanoferrate(II) to hexacyanoferrate(III) on interdigitated microarray electrodes. A characteristic dependence on the magnetic field direction was observed. Using a unique feature of the microarray electrode, an attempt was made to obtain a new method to analyze the components of the flux, and a hopeful way was shown to apply these microarray electrodes in a magnetic field.

Interdigitated array electrodes (IDAEs)[1—3] have great potential as a micro-sensor for electrochemical detection. In this work, the basic electrochemical behaviors of interdigitated array-shaped Pt electrodes in a magnetic field parallel to the electrode surface were studied in terms of electrochemistry and magneto-hydrodynamics. Also the present work to the best of our knowledge is the first to report on the high magnetic field effect on an interdigitated array electrode (IDAE). All of the IDAEs[1—3] used in this study were designed by the NTT group[1] and are commercially available. IDAEs have been suggested due to their availability, especially for electrochemical micro-sensors[1c—1f,2,3] for the HPLC detection of small amounts bio-materials, since Matsue et al.[2] have used IDAEs in flowing a solution for detecting bio-materials for the first time. The characteristic feature of IDAE is "Redox Cycling",[1] which is a new tool for obtaining a steady state current without spherical diffusion.

Magnetic field effects on chemical and physical processes have often been discussed over the past several decades.[4,5] Recently, high and various types of magnetic fields can be utilized with the evolution of superconducting magnets. Especially, using 1 Tesla (T) or higher magnetic fields, novel and interesting behaviors have been reported.[6—9] During the last several decades, microelectrodes[10] have also received much attention by electrochemical researchers not only for basic studies, but also for various applications. Ragsdale et al.[8] and Leventis et al.[11] had already reported on magnetic-field effects in high magnetic fields[8a] or 1—2 T magnetic fields[8b—8d,11] for electrochemical reactions on micro-[8] or milli-[11] disk electrodes. Our attempt to use IDAEs means finding the relationship between the directions of diffusion and the magnetic flux with non-spherical processes, but in lower dimensions, cylindrical or planar diffusion processes. To use the IDAEs in a magnetic field also means finding a new class of micro-sensors.

Experimental

1. Setup of IDA Electrodes and the Preparation of an Electrochemical Cell. All IDAEs were purchased (2048, BAS Inc., Japan) and the IDAE was constructed with 4 platinum electrode patterns on a small quartz plate. Two of them were interdigitated (10 μm width, 5 μm gap, 2 mm length, 65 pairs of microarrays) and the other two were large, auxiliary and quasi-reference electrodes, respectively. Using these two interdigitated electrodes at different potentials (it is called "dual mode"; one array works as an anode and the other works as a cathode), "redox cycling"[1f] occurs and the limiting current increases by several times more than that for those cases using only one interdigitated electrode (it is called "single mode"; one array is used for a working electrode and the other is disconnected from the system). All chemicals were of reagent grade and were used as received. Water was purified using a WP-500 (Millipore-Yamato, Japan). The sample solution was a 1×10^{-3} mol dm^{-3} potassium hexacyanoferrate(II) ($K_4Fe^{II}(CN)_6$) aqueous solution with 0.2 mol dm^{-3} sodium sulfate as the supporting electrolyte. In a flow system, IDAEs are said to work as multiple dual-channel flow electrodes,[12] which generate a steady state by redox cycling; however, in the single mode, an IDAE is said to work as a single-channel flow electrode; which generates a quasi-steady state. The electrochemical cell was made with 0.7 mm thick glass plates, a viton O-ring and an interdigitated array (IDA) pattern-deposited 0.5 mm thick quartz plate (Fig. 1(a)). A kind of Acrylic polymer was brushed on the surface of the electrode after

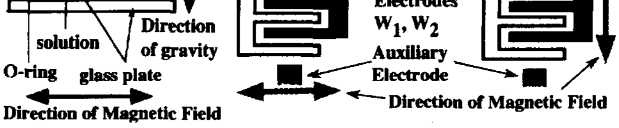

Fig. 1. Electrochemical cell (a) and IDAE. (b1) in parallel configuration (Case 1, direction A) and (b2) in perpendicular configuration (Case 2, direction B).

washing with acetone to keep only the array appearing; the remaining area was covered and dried overnight. The sample solution (ca. 0.4 mL) was put into the cell (see Fig. 1(a)) with a syringe.

2. Electrochemical Measurements. A helium-free cryogenic superconducting magnet (HF-10-100VHT, Sumitomo Heavy Industries, Ltd., Japan) was placed horizontally and the sample cell was put in the center of a magnetic field. The IDA plate was placed facing downward (the direction for decreasing natural convection), and the directions of the arrays were parallel (Fig. 1(b1): Case 1) or perpendicular (Fig. 1(b2): Case 2) to the magnetic field. On the other hand, the direction of the magnetic field is defined as directions A (in Case 1) and B (in Case 2), respectively. An electrochemical measurement was carried out at room temperature with a dual potentiostat (DPGS-1S-S, Nikko Keisoku Co., Japan). At first, one of the twin IDAEs (W_1) was set at 0 V, and the other (W_2) was disconnected. W_1 was then set at 0.5 V and the anodic current measured in the single mode (I_s) or W_1 and W_2 were set at 0.5 and −0.1 V, respectively, and the anodic and cathodic current measured in the dual mode (I_d). The specific electrochemical reactions are as follows:

$$\mathrm{Fe(CN)_6{}^{4-}} \rightarrow \mathrm{Fe(CN)_6{}^{3-}} + e^- \qquad \text{(at anode : } W_1\text{)}, \qquad (1)$$

$$\mathrm{Fe(CN)_6{}^{3-}} + e^- \rightarrow \mathrm{Fe(CN)_6{}^{4-}} \qquad \text{(at cathode : } W_2\text{)}. \qquad (2)$$

The magnetic flux density (B) was first raised from 0 to 10 T, and then gradually reduced, while the intensity of the magnetic field was maintained during the measurement.

3. Expectation for Comprehending the Ionic Flow in a Magnetic Field. The Lorentz (magneto-hydrodynamic: MHD) force is described by

$$\boldsymbol{F} = \boldsymbol{J} \times \boldsymbol{B}, \qquad (3)$$

where $\boldsymbol{F}$ is the Lorentz (MHD) force, $\boldsymbol{J}$ is the total ionic flux vector (i.e., the electric current) and $\boldsymbol{B}$ is the magnetic flux density vector ($|\boldsymbol{B}| = B$).

With the effect of the Lorentz (MHD) force, the ionic flux causes rotation. For each case, in the presence of a magnetic field in directions A (Case 1, Fig. 1(b1)) and B (Case 2, Fig. 1(b2)), the ionic flux is supposed to change direction. The expected features are shown in Figs. 2 and 3.

The thick solid black arrows and symbols denoted by the letter "B" in the figures show the magnetic-field direction, the thin solid black arrows labeled by the letter "*i*" correspond to the current, and the solid dark gray arrows labeled by the letter "F" shows the direction of the MHD force. The sizes of the arrows and symbols have no specific meanings (they show only the directions of the factors), because we know nothing about the components of the flux in the sample solutions. One of our objectives was to obtain information about the components of the flux in order to characterize the IDAE in a magnetic field. Surveys of the flux in the single mode for Cases 1 and 2 are shown in Figs. 2(a) and 2(b). The surveys of the flux in the dual mode, in the absence of a magnetic field, Cases 1 and 2, are shown in Figs. 3(a), 3(b), and 3(c), respectively. In Fig. 2(b), all of the "F"s point in the same direction and, contrary to Fig. 2(b), the directions of the "F"s are different at the edge of the electrode in Fig. 2(a). In Fig. 3(a), the established flows in the "Redox Cycling" are shown. In the presence of a magnetic field, in Case 1, the "F"s are expected to alter the directions of the "Redox Cycling", as shown in Fig. 3(b). In Fig. 3(c), the expected "F"s are in different directions (alternate), and should be less effective due to the solution resistance.

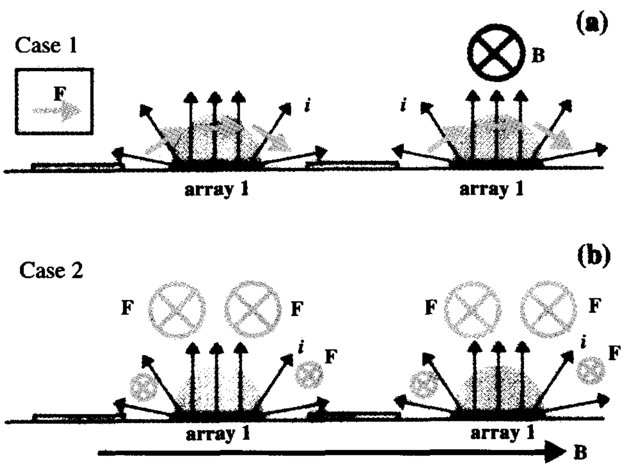

Fig. 2. Schematic illustrations of the ionic flows on IDAE. (a) Case 1 and (b) Case 2. Black arrows indicate the current (*i*), the arrows and the symbols denoted by the thick black line (**B**) indicate the direction of the magnetic field, and the gray arrows and symbols (**F**) indicate the directions of the Lorentz (MHD) force.

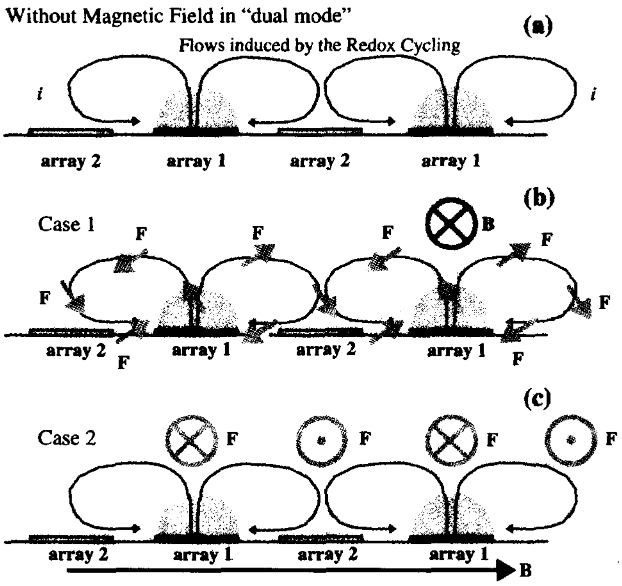

Fig. 3. Schematic illustrations of the ionic flows on IDAE. (a) Ionic flows caused by the "Redox Cycling" in the absence of the magnetic field, (b) Case 1 and (c) Case 2.

Results and Discussion

1. Results of a Current Change in a Magnetic Field. In each (single or dual) mode, the anodic current (I_s, I_d) was determined; the results are shown in Fig. 4. The change in the single mode for Case 1 was smaller than that in Case 2, though the change in the dual mode in Case 1 was larger than that in Case 2. IDA behaved as usual and the I_d value was 10 or more times larger than that in the single mode (the ionic flux should also be). The current ratio in the magnetic field ($I_R = I_B/I_0$) was calculated from the current without a magnetic field (I_0) and the current with a magnetic field (I_B). To standardize the values, we calculated I_R. As the

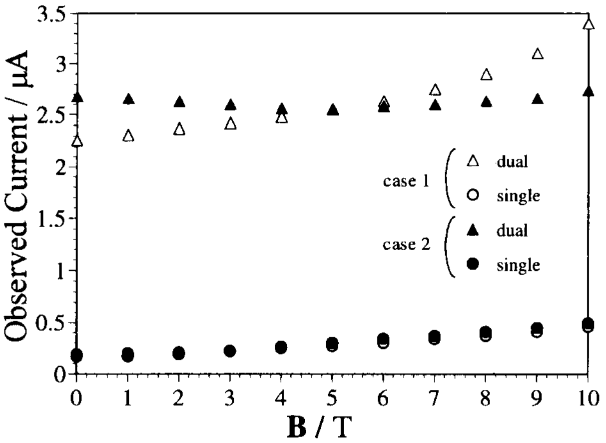

Fig. 4. Change in the observed current. Observed currents (I_s, I_d) in single mode (in Case 1, (○) and in Case 2, (●)) and in dual modes (in Case 1, (△) and in Case 2, (▲)). (Case 1 is in parallel configuration and Case 2 is perpendicular.)

acrylic polymer was brushed by hand, the electrode area was different each time. The I_R change (ΔI_R) is described by

$$\Delta I_R = I_R - 1 = \frac{I_B - I_0}{I_0}. \qquad (4)$$

Similar to HPLC[1c—1f] and a flow system,[2,3] in a higher magnetic field the collection efficiency was lower.[1a,1e,2,3] Each value of ΔI_R is shown in Fig. 5. In Figs. 4 (observed current values) and 5 (the enhancement results), the symbols are assigned in the figure captions.

The ratio I_d/I_s, is called the "Redox Cycling" number, and in our cases the normalized values of I_d/I_s are shown in Fig. 6. The result of Case 2 is shown by the symbol (●) and the results of Case 1 are shown by the symbols (○,○). The gray-lined open circle (○) is same as the black-lined open circle (○), and is drawn in a different scale (upper X-axis) from the two other symbols (lower X-axis). The anisotropic data are shown in Fig. 7. It is the ratio $I_{//}/I_{\perp}$ ($I_{//}/I_{\perp}$; the symbols, $\perp$ means Case 2, and // means Case 1) for each of the single (○) and dual (●) modes. Considering their values, we would be able to estimate the difference in the components of the flow in the magnetic field.

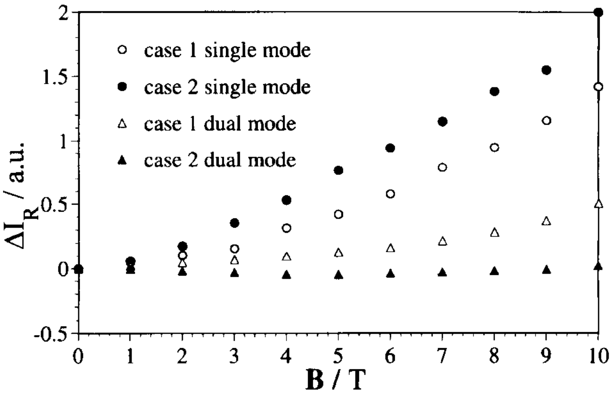

Fig. 5. Change in the current enhancement. Current ratio changes (ΔI_R) in single mode (in Case 1, (○) and in Case 2, (●)) and in dual modes (for Case 1, (△) and for Case 2, (▲)). (Case 1 is in parallel configuration and Case 2 is perpendicular.)

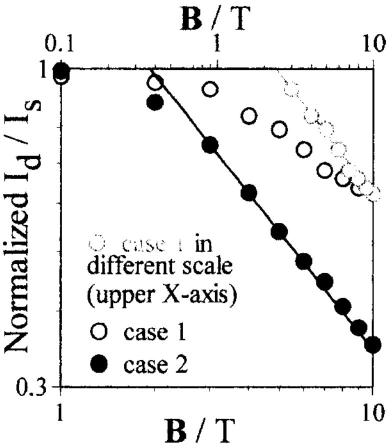

Fig. 6. Change in normalized "Redox Cycling". (a) Normalized I_d/I_s in Case 1 (○), for Case 2 (●) and in ×10 x-scale (0.1—10) for Case 1 (○). The line (······) on Case 1 (○) is drawn parallel to the line (——) for Case 2 (●) (fitted for 3—10 T).

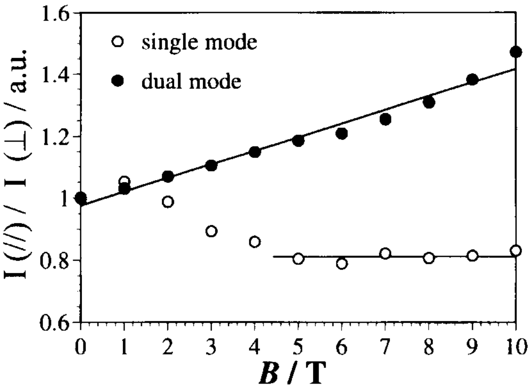

Fig. 7. Change in anisotropic data ($I_{s\text{ or }d,//}/I_{s\text{ or }d,\perp}$). The symbols correspond to (●: single mode) and (○: dual mode). The straight line on ○ is $(I_{s,//}/I_{d,\perp}) = 0.044T + 0.98$.

2. Single Mode (1). Case 1 (Direction A). The current was enhanced with an increase in the magnetic flux density (Figs. 4 and 5). The current enhancement (ΔI_R) was low in the 0—3 T region, and ΔI_R increased more in the high magnetic flux density 3—5 T region, while beyond 5 T, ΔI_R was as high as the slope in the single mode in Case 2 (see next paragraph). In this case (Case 1 in single mode (○) in Fig. 5), the correlation between ΔI_R and B was found to be

$$\Delta I_R \propto B^x \qquad (x \approx 2.1). \qquad (5)$$

This is slightly larger than the typical values obtained from previous studies ($x = 0.25$—1.6).[13,14] It seemed to originate from the difference in the electrode shape and its diffusion layer (cylindrical, planar or spherical).

3. Single Mode (2). Case 2 (Direction B). In Case 2, the current enhancement (ΔI_R) was a slightly larger than in Case 1 in the low magnetic flux-density region. Beyond 5 T, the results of Case 1 and Case 2 seem to be parallel in Fig. 5. The difference was supposed to be due to the difference of the total amount of the ionic flux which we mentioned in Exp.3, Figs. 2(b) and 3(c). With each direction (Case 1 = parallel or Case 2 = perpendicular) of the flux, the ionic current should be raised, because it works as "a single channel flow electrode".[12]

4. Dual Mode (1). Case 1 (Direction A). In Case 1, the current change was not very small, but the current enhancement (ΔI_R) was smaller than the enhancement in the single mode. The change in the current is shown in Fig. 4 and the ΔI_R is shown in Fig. 5. A slight increase was seen only in high magnetic-field region.

5. Dual Mode (2). Case 2 (Direction B). In Case 2, the current change was small and no significant change was seen in the current enhancement (ΔI_R). The change in the current is shown in Fig. 4 and the ΔI_R is shown in Fig. 5. No significant increase was seen in the all regions from 0 to 10 T, while a slight decrease was seen near 5 T. In this case, the magnetic field had no effect on the dual mode.

6. From the Results of Both Modes for Case 1 and Case 2. In Fig. 5, I_s (● : Case 2) has a good linearity to B for determining in the upper 3 T high magnetic field; on the other hand, I_d (△ : Case 1) was not significantly changed and could be used as a reference. These tendencies will be helpful for detecting B in the higher region.

7. "Redox Cycling". We used the normalized value of (I_d/I_s), because the slopes and the features were the same with normalized or not. If it is possible to compare our results on the **B** (T) scale with the flow-system results[1d,1e] in "volume flow rate (ml min^{-1})", our results on a log–log scale are shown in Fig. 8. In Case 1, the features are similar to the results in a thin-layer cell (12—50 μm); in Case 2, its features are similar to the results in a thick cell (ca. 125 μm). The volume flow rate in the dual mode is much lower than the result in Case 1. Both of our results seemed to be in the "quasi-amperometric region" (the region of small volume flow rate). From the unique characteristics of IDAE, only the perpendicular component of the flow to the long side of the arrays (direction B) is effective for "redox cycling";[1g] also the slopes are independent of the dimensions of the array and layer thickness and almost the same as a function of the "volume flow rate" in the quasi-amperometric region.[1f] This tells us that the actual (effective) perpendicular component (direction B) of **J** in Case 1 (○) is about one tenth of that in Case 2 (●). For example, $a \times 10$ change in Case 2 is compatible to $a \times 100$ change in Case 1 as the "volume flow rate".[1f] Although there is no more information about the real values on the x-axis as the "volume flow rate",[1f] it will show some keys to analyze **J** in order to calculate Eq. 5. It is not strange and it is reasonable, based on our expectation (see Exp. 3.). In Case 1, almost all of the components should be parallel (in direction A), that should not be effective for the "Redox Cycling". With these kinds of analyses, the inconvenience of the complex diffusion process of IDAE should be overcome. Even if it is not suitable for estimating the flow components only from the total flow volume, the value for the Case 2 dual mode can be used as the standard value, which is not responsible for the MHD effect. It is a unique feature for electrochemical detection in a magnetic field.

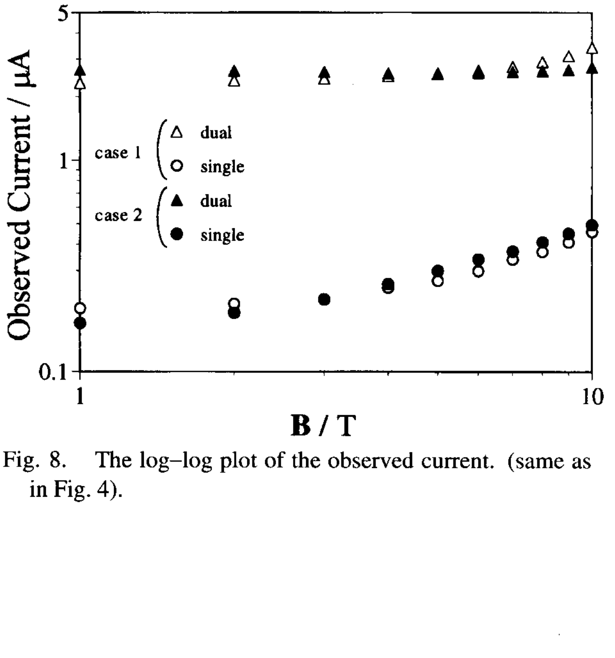

Fig. 8. The log–log plot of the observed current. (same as in Fig. 4).

8. Anisotropic Data. The anisotropic values were calculated and are shown in Fig. 7. In Fig. 7, the value in the single mode ($I_{s,//}/I_{s,\perp}$: ●) and that in the dual mode ($I_{d,//}/I_{d,\perp}$: ○) are shown. A clear difference was seen between them. The ($I_{s,//}/I_{s,\perp}$) value decreased in the interval from 0 to 5 T. Beyond 5 T, the ($I_{s,//}/I_{s,\perp}$) value seemed to be constant (ca. 0.82). This should come from the difference in both cases (the edge part of the IDA). Another possible reason is the change in the MHD flow pattern for a higher B. The value of ($I_{d,//}/I_{d,\perp}$) increased linearly.

9. In the Lower Magnetic Flux Density Region (0—3 T). A threshold[8,12,13] or a slight decrease[8b] was found for every case in the interval from 0 to ca. 3 T (Fig. 5). These are similar phenomena that were observed by Ragsdale et al.[8] for the nitrobenzene reduction in a magnetic field. They suggested that the threshold corresponds to the minimum value of the magnetic force which is necessary to observe the limiting current enhancement[8d] that starts or keeps the ionic flow against the solution resistance. They also suggested that the threshold is caused by a change in the homogeneity of the magnetic field beyond ca. 1 T.[8]

10. The Dependence of $(I_{s,d})^{-1}$ vs. $(|I_{s,d}|B)^{-0.25}$. If we apply Eq. 6[15] to our IDAE results for estimating the current dependence for the MHD effect,

$$\frac{1}{I} - \frac{1}{I_k} = \frac{1}{H^{*1.25} C_0 (IB)^{0.25}}, \tag{6}$$

where H^* is a constant and C_0 is the concentration of the substance.

The results of calculations for the single mode and the dual mode are shown in Figs. 9(a) and 9(b), respectively. The x-axis is $(|I\,|B)^{-0.25}$ ((T μA 1.3 mm^{-2})$^{-0.25}$) and the y-axis is I^{-1} (μA^{-1} 1.3 mm^2). With these results in the single mode, the slopes in the high magnetic-field region (beyond 3 T) vary in a similar way. Both slope values were 0.18. In the usual case, the I_k has some positive value, called the "the reaction current", or is nearly equal to zero in a diffusion-limited

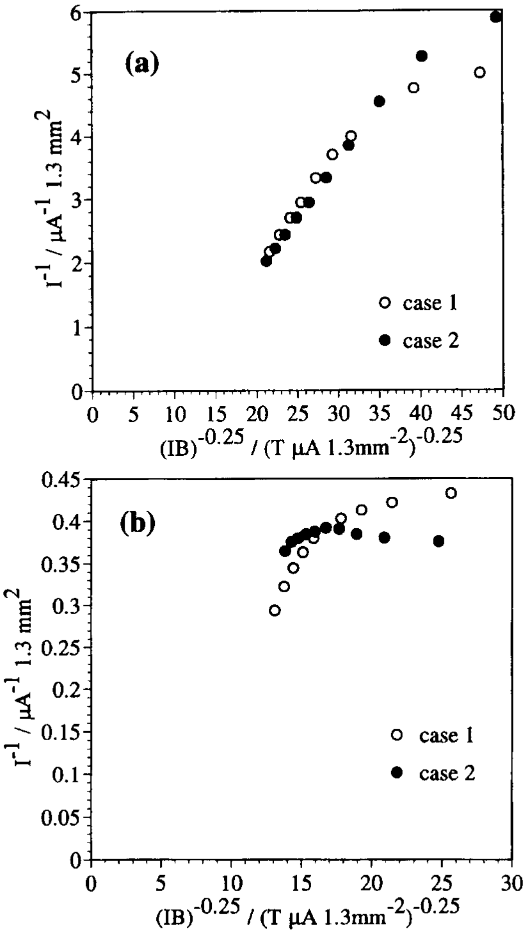

Fig. 9. The dependence of I^{-1} on $(|I|\,|B|)^{-0.25}$. (a) The calculated values of Case 1 (○) and Case 2 (●) in the single mode. (b) The calculated values of Case 1 (○) and Case 2 (●) in the dual mode.

process. However in our cases, both in the single mode and Case 1 in the dual mode, they were negative values. This shows that other unknown factors are included in our IDAE cases. Contrary to the other cases, the calculation values in Case 2 in the dual mode was almost constant, showing that the current is not responsible for the MHD effect.

Conclusions

Based on these results, we found some new useful characteristics of IDAEs in a high magnetic field. Under the present conditions, the dependence of the current enhancement in a magnetic field had good linearity to the magnetic flux density, *B*, in the interval from 5 to 10 T. This would be advantageous over other kinds of microelectrodes, because their responses are not linear in the interval 5 to 10 T. The possibility of a deconvolution of the ionic flux components in the magnetic flux density, which is difficult to predict by calculations involving the present situation, was shown using "the redox cycling", the very characteristics of IDAE. These characteristics would compensate for any inconvenience concerning the complexity of the IDAE's diffusion process. With the IDAEs, we think our future work will be to determine the distinction between the MHD effect and the effect of the magnetic force as well as verifying their assignments in more-homogeneous or less-homogeneous magnetic field in Case 1 or Case 2 to the electrode surface. As with the IDAE, it is highly possible to control the direction of the diffusion near to the electrode surface and it is important to compare the difference between the spherical and the cylindrical or planar diffusion processes.

References

1 a) K. Aoki, M. Morita, O. Niwa, and H. Tabei, *J. Electroanal. Chem.*, **256**, 269 (1988). b) O. Niwa, M. Morita, and H. Tabei, *Anal. Chem.*, **62**, 447 (1990). c) H. Tabei, M. Takahashi, S. Hoshino, O. Niwa, and T. Horiuchi, *Anal. Chem.*, **66**, 3500 (1994). d) S. Hoshino, O. Niwa, H. Tabei, M. Takahashi, and M. Morita, *Denki Kagaku*, **64**, 195 (1996). e) M. Takahashi, M. Morita, O. Niwa, and H. Tabei, *J. Electroanal. Chem.*, **335**, 253 (1992). f) M. Morita, O. Niwa, and T. Horiuchi, *Electrochim. Acta*, **42**, 3177 (1997). g) T. Matsue and M. Morita, "New Collection of Techniques in Electrochemistry (2)," The Electrochemical Society of Japan, Tokyo (1995).

2 a) T. Matsue, A. Aoki, T. Abe, and I. Uchida, *Chem. Lett.*, **1989**, 133. b) T. Matsue, A. Aoki, E. Ando, and I. Uchida, *Anal. Chem.*, **62**, 407 (1990). c) A. Aoki, T. Matsue, and I. Uchida, *Anal. Chem.*, **62**, 2206 (1990).

3 K. Aoki and H. Matsuda, *J. Electroanal. Chem.*, **94**, 157 (1978).

4 T. Z. Fahidy, *J. Appl. Electrochem.*, **13**, 553 (1983).

5 R. A. Tacken and L. J. J. Janssen, *J. Appl. Electrochem.*, **25**, 1 (1995), and references cited therein.

6 F. Kimura, T. Kimura, A. Sugisaki, M. Komatsu, H. Sata, and E. Ito, *J. Polym. Sci., Part B, Polym. Phys.*, **35**, 2741 (1997).

7 Y. Ikezoe, N. Hirota, J. Nakagawa, and K. Kitazawa, *Nature*, **393**, 749 (1998).

8 a) S. R. Ragsdale, K. M. Grant, and H. S. White, *J. Am. Chem. Soc.*, **120**, 13461 (1998). b) S. R. Ragsdale and H. S. White, *Anal. Chem.*, **71**, 1923 (1999). c) S. R. Ragsdale, J. Lee, and H. S. White, *Anal. Chem.*, **69**, 2070 (1997). d) J. Lee, S. R. Ragsdale, X. Gao, and H. S. White, *J. Electroanal. Chem.*, **422**, 169 (1997).

9 S. Mori, M. Kumita, and M. Takeuchi, "Transfer Phenomena in Magnetohydrodynamic and Electroconducting Flows," Kluwer Academic Pub., Dordrecht, Netherlands (1998).

10 K. Aoki, *Electroanalysis*, **5**, 627 (1993), and references cited therein.

11 N. Leventis, M. Chen, X. Gao, M. Canalas, and P. Zhang, *J. Phys. Chem. B*, **102**, 3512 (1998).

12 K. Aoki and H. Matsuda, *J. Electroanal. Chem.*, **94**, 157 (1978).

13 R. Aogaki, K. Fueki, and T. Mukaibo, *Denki Kagaku*, **43**, 504 (1975).

14 O. Aaboubi, J. P. Chopart, J. Douglade, and A. Olivier, *J. Electrochem. Soc.*, **137**, 1796 (1990).

15 R. Aogaki, *Chem. Ind.*, **48**, 788 (1997).